Molecular Pharmacology Fast Forward. Published on May 2, 2016 as DOI: 10.1124/mol.116.103358
This article has not been copyedited and formatted. The final version may differ from this version.

TITLE PAGE

Use-dependent Block of Human Cardiac Sodium Channels by GS967

Franck Potet, Carlos G. Vanoye, and Alfred L. George, Jr.

Department of Pharmacology, Northwestern University Feinberg School of Medicine, Chicago, IL 60611

RUNNING TITLE PAGE

GS967 Block of Human Cardiac Sodium Channels

To whom correspondence should be addressed:
Alfred L. George, Jr.
Department of Pharmacology
Northwestern University Feinberg School of Medicine
Searle 8-510
320 East Superior Street
Chicago, IL 60611
Tel: 312-503-4893
al.george@northwestern.edu

The number of text pages: 32
Number of tables: 1
Number of figures: 8
Number of references: 32
The number of words in the *Abstract:* 247
The number of words in the *Introduction*: 449
The number of words in the *Discussion*: 951

ABBREVIATIONS

Na_V: voltage gated sodium channel
GS967: GS-458967
ATX-II: Anemonia sulcata toxin II
UDB: use-dependent block
D4: domain 4
LA: local anesthetics
I_{NaP}: peak sodium current
I_{NaL}: late sodium current
S4: segment 4
S6: segment 6
DMEM: Dubelcco's modified eagle medium
FBS: fetal bovine serum
GFP: green fluorescent protein
LQTS: long QT syndrome
APD: action potential duration
IRES: internal ribosome entry site
OD: outer diameter
BAPTA: 1,2-bis(o-aminophenoxy)ethane-N,N,N',N'-tetraacetic acid
HEPES: 4-(2-hydroxyethyl)-1-piperazineethanesulfonic acid

Molecular Pharmacology Fast Forward. Published on May 2, 2016 as DOI: 10.1124/mol.116.103358
This article has not been copyedited and formatted. The final version may differ from this version.

TTX: tetrodotoxin
CMV: cytomegalovirus
U.S.A.: United States of America
SEM: standard error of the mean
WT: wildtype
IC_{50}: half maximal inhibitory concentration
($V_{½}$): half activation/inactivation voltage
ATX-II: Anemone toxin II
ERP: effective refractory period
EAD: early after depolarization
DAD: delayed after depolarization
PRR: post-repolarization refractoriness
HEK-293: human embryonic kidney 293 cells
tsA201: transformed human embryonic kidney 293 cells

Molecular Pharmacology Fast Forward. Published on May 2, 2016 as DOI: 10.1124/mol.116.103358
This article has not been copyedited and formatted. The final version may differ from this version.

ABSTRACT

GS967 is a recently described novel sodium channel inhibitor exhibiting potent antiarrhythmic effects in various *in vitro* and *in vivo* models. The antiarrhythmic mechanism has been attributed to preferential suppression of late sodium current. However, there has been no reported systematic investigation of the effects of this compound on isolated sodium channels. Here, we examined the effects of GS967 on peak (I_{NaP}) and late (I_{NaL}) sodium current recorded from cells that heterologously expressed human $Na_V1.5$, the principle cardiac sodium channel. As previously described, we observed that GS967 exerted tonic block of I_{NaL} (63%) to a significantly greater extent than I_{NaP} (19%). However, GS967 also caused a reduction of I_{NaP} in a frequency-dependent manner consistent with use-dependent block (UDB). GS967 evoked more potent UDB of I_{NaP} (IC_{50}=0.07μM) than ranolazine (16μM) and lidocaine (17μM). Use-dependent block was best explained by a significant slowing of recovery from fast and slow inactivation with a significant enhancement of slow inactivation in the presence of GS967. Further, GS967 was found to exert these same effects on a prototypical long-QT syndrome mutation (delKPQ). An engineered mutation at an interaction site for local anesthetic agents (F1760A) partially attenuated the effect of GS967 on UDB, but had no effect on tonic I_{NaL} block. We conclude that GS967 is a preferential inhibitor of I_{NaL}, but it also exerts previously unreported strong effects on slow inactivation and recovery from inactivation resulting in substantial UDB that is not entirely dependent on a known interaction site for local anesthetic agents.

Molecular Pharmacology Fast Forward. Published on May 2, 2016 as DOI: 10.1124/mol.116.103358
This article has not been copyedited and formatted. The final version may differ from this version.

INTRODUCTION

Sodium current (I_{Na}) in cardiac myocytes carried primarily by $Na_V1.5$ channels is responsible for the rapid upstroke of atrial and ventricular action potentials as well as the rapid propagation of depolarization throughout the heart. When $Na_V1.5$ fails to inactivate fully after opening, Na^+ influx continues throughout the action potential plateau. The resulting current, referred as late I_{Na} (I_{NaL}), can promote prolongation of the action potential duration. Late I_{Na} is normally small but its amplitude is greater in certain acquired or heritable conditions, including failing and/or ischemic heart (Le Grand et al., 1995), oxidative stress (Song et al., 2006), or mutations in *SCN5A*, which encodes $Na_V1.5$ (Bennett et al., 1995; Ruan et al., 2009). *SCN5A* mutations that cause enhanced I_{NaL} produce type 3 long QT syndrome (LQT3) characterized by a high propensity for life threatening ventricular arrhythmia torsades de pointes and may also contribute to atrial fibrillation (Antzelevitch et al., 2014).

Preferential inhibition of I_{NaL} improves electrical function in myocytes isolated from failing and ischemic hearts or that have been exposed to cardiac glycosides, hydrogen peroxide, enhancers of I_{NaL}, or drugs that block hERG current (I_{Kr}) and reduce repolarization reserve (Le Grand et al., 1995; Maltsev and Undrovinas, 2008; Sicouri et al., 1997; Song et al., 2008; Song et al., 2006; Song et al., 2004; Sossalla et al., 2010; Wu et al., 2011). Many local anesthetic and antiarrhythmic agents have greater potency to block I_{NaL} than peak I_{Na} (I_{NaP}). Certain compounds such as ranolazine (Gupta et al., 2015) and F15845 (Pignier et al., 2010), are described as preferential I_{NaL} blockers.

Molecular Pharmacology Fast Forward. Published on May 2, 2016 as DOI: 10.1124/mol.116.103358
This article has not been copyedited and formatted. The final version may differ from this version.

GS967 (a triazolopyridine derivative, 6-(4-(trifluoromethoxy)phenyl)-3-(trifluoromethyl)-[1,2,4]triazolo[4,3-a]pyridine)(Koltun et al., 2016) is a recently described sodium channel blocker that was originally demonstrated to exert potent antiarrhythmic effects in rabbit ventricular and canine atrial myocytes by a proposed mechanism of action involving preferential I_{NaL} block (Belardinelli et al., 2013; Sicouri et al., 2013). More recently, GS967 has been shown to suppress arrhythmogenicity evoked by ischemia (Bonatti et al., 2014), hypokalemia (Pezhouman et al., 2014) and catecholamines (Alves Bento et al., 2015) in canine and porcine models. In each of these reports, the effect of GS967 was ascribed to preferential block of I_{NaL}. Given these promising effects of GS967, a more comprehensive analysis of its biophysical effects on human cardiac sodium channels is warranted.

In this study, we investigated the molecular pharmacology of GS967 on heterologously expressed human $Na_V1.5$. In addition to preferential block of I_{NaL}, we observed a previously unreported and potent use-dependent block of I_{NaP}. Use-dependent block of $Na_V1.5$ by GS967 stems from its ability to impair recovery from inactivation and to enhance entry into slow inactivated states. We suggest that these previously unrecognized properties of GS967 may contribute to its antiarrhythmic effects.

Molecular Pharmacology Fast Forward. Published on May 2, 2016 as DOI: 10.1124/mol.116.103358
This article has not been copyedited and formatted. The final version may differ from this version.

MATERIALS AND METHODS

Plasmid constructs, cell culture and transfection

Plasmids encoding human $Na_V1.5$ and the $Na_V1.5$ mutants delKPQ and F1760A were sub-cloned into the pRcCMV mammalian expression vector. Channel constructs were then co-transfected with a plasmid encoding green fluorescent protein (GFP) alone or one with the human sodium channel β1 subunit in series with an IRES element and GFP as fluorescent markers of transfected cells. The complete coding regions of all plasmid constructs were verified by Sanger sequencing before use in experiments. Cultured cells (tsA201) were transiently transfected with 1.5 μg of pRCCMV-$Na_V1.5$ (or mutants) and 1 μg of pEGFP-IRES or pEGFP-IRES-hβ1 using Lipofectamine™ (Thermo Fisher Scientific, Waltham, MA) according to the manufacturer's instructions. The tsA201 cells were grown in DMEM medium supplemented with 10% fetal bovine serum and penicillin (50 units·ml^{-1}) / streptomycin (50 μg·ml^{-1}) at 37°C in 5% CO_2. Green or red fluorescent cells were selected for electrophysiological analysis 24-48 hours after transfection. In all experiments, the β1 subunit was co-expressed with $Na_V1.5$ except where mentioned. $Na_V1.5$ was also stably expressed in HEK-293 cells and maintained in the same media plus G418 (500 μg/ml).

Electrophysiology

Sodium currents in transiently transfected tsA201 cells were recorded at room temperature 24-48 hours after transfection using the manual whole-cell patch clamp technique. Patch-clamp pipettes were pulled from thin-wall borosilicate glass (OD: 1.5

Molecular Pharmacology Fast Forward. Published on May 2, 2016 as DOI: 10.1124/mol.116.103358
This article has not been copyedited and formatted. The final version may differ from this version.

mm, Warner Instrument Corp., Hamden, CT, U.S.A.) on a P-1000 multistage Flaming/Brown micropipette puller (Sutter Instruments, Novato, CA, U.S.A) and fire polished to a resistance between 1.0 and 2.5 MΩ. In order to avoid the time-dependent shift of the I_{Na} availability curve commonly observed during patch-clamp experiments, voltage-dependent inactivation was always assessed within 2 minutes after cell membrane rupture. The holding potential for all experiments -120 mV and specific voltage-clamp protocols are depicted as figure insets. The pipette solution used contained (in mM): 10 NaF, 100 CsF, 20 CsCl, 20 BAPTA, 10 HEPES, adjusted to pH 7.35 with CsOH. The extracellular (bath) recording solution contained (in mM): 145 NaCl, 4 KCl, 1 $MgCl_2$, 10 HEPES, and 1.8 $CaCl_2$, adjusted to pH 7.35 with CsOH. Series resistance was compensated 80%. Data acquisition was carried out using an Axopatch 200B patch clamp amplifier and pCLAMP 10.0 software (Molecular Devices, Sunnyvale, CA). A Boltzmann function ($I = 1/[1 + \exp(V_t - V_{1/2})/k)]$) was fitted to the availability and activation curves to determine the membrane potential eliciting half-maximal activation/inactivation ($V_{1/2}$), where k is the slope factor. All data were analyzed using pCLAMP 10.0 or Microsoft Excel 2007 and plotted using SigmaPlot 10.0 (Systat Software, Inc., San Jose, CA). Experiments examining late I_{Na} and ramp-currents utilized tetrodotoxin (TTX; Tocris Bioscience, Bristol, UK) to allow for the determination of TTX-sensitive sodium current. TTX was added to the bath solution from a 3 mM stock solution of TTX (in water) to a final concentration of 10 µM. TTX was applied at the end of the protocol right after GS967. TTX-sensitive current was then determined by offline digital subtraction.

Molecular Pharmacology Fast Forward. Published on May 2, 2016 as DOI: 10.1124/mol.116.103358
This article has not been copyedited and formatted. The final version may differ from this version.

Automated patch clamp recording

Automated patch clamp recording was performed using a Syncropatch 384 PE (Nanion Technologies, München, Germany). Pulse generation and data collection were done with PatchController384 V.1.3.0 and DataController384 V1.2.1 (Nanion Technologies). Whole-cell currents were filtered at 3 kHz and acquired at 10 kHz. The access resistance and apparent membrane capacitance were estimated using built-in protocols. Series resistance was compensated 95% and leak and capacitance artifacts were subtracted out using the P/4 method. The average seal resistance was 1.01 ± 0.04 GΩ, and cells were excluded from analysis if the current at the holding potential (–120 mV) was >10 % of the peak current.

HEK-293 cells stably expressing Nav1.5 were plated into 100 mm culture dishes 48-72 hours prior to the experiment. The day of the experiment, cells (60-80% confluency) were washed once with PBS (-Mg/Ca), detached with trypsin and re-suspended in culture media and external solution at 180,000 cells/ml. Cells were allowed to recover for at least 30 min at 15 °C while shaking on a rotating platform. Following equilibration, 10 µl of cell suspension was added to each well of a 384-well, single-hole, low resistance (2 MΩ) 'chip' (Nanion Technologies). Whole-cell currents were recorded at room temperature in the whole-cell configuration. The external solution contained (in mM) the following: NaCl 140, KCl 4, $CaCl_2$ 2, $MgCl_2$ 1, HEPES 10, glucose 5, pH = 7.4). And the internal solution contained (in mM) the following: CsF 110, CsCl 10, NaCl 10, HEPES 10, EGTA 10, pH = 7.2.

Molecular Pharmacology Fast Forward. Published on May 2, 2016 as DOI: 10.1124/mol.116.103358
This article has not been copyedited and formatted. The final version may differ from this version.

Data analysis

Patch-clamp measurements are presented as the means ± SEM. Comparisons were made using Student's *t*-test with $P < 0.05$ considered significant.

Molecular Pharmacology Fast Forward. Published on May 2, 2016 as DOI: 10.1124/mol.116.103358
This article has not been copyedited and formatted. The final version may differ from this version.

RESULTS

Preferential late I_{Na} block of human $Na_V1.5$ by GS967

We examined the effects of 1 μM GS967 on I_{NaP} and I_{NaL} recorded from tsA201 cells transiently expressing wildtype (WT) human $Na_V1.5$ in the presence of the β1 subunit. As previously reported (Belardinelli et al., 2013), we found that 1 μM GS967 at a slow pulsing rate (0.2 Hz) inhibited I_{NaL} to a significantly greater extent than I_{NaP} (62% vs 18.6% inhibition respectively, $P < 0.001$; Fig. 1A and C). This differential inhibitory effect of GS967 on I_{NaP} and I_{NaL} was also observed in cells expressing $Na_V1.5$ in the absence of the β1 subunit (Supplemental Fig. S1). GS967 caused a significant 4 mV hyperpolarizing shift in the $V_{½}$ of activation but it did not modify the inactivation kinetics (Supplemental Fig. S2). GS967 also appeared to cause a significant shift in the $V_{1/2}$ of steady-state inactivation from -83.2 ± 0.8 mV to -95.3 ± 1.4 mV ($P < 0.001$; n = 18). To exclude the confounding effects of time-dependent shifts in steady-state inactivation known to occur with $Na_V1.5$, we examined two separate groups of cells exposed to control (drug free) conditions or GS967 at a fix time interval following establishment of the whole-cell seal. We found that GS967 does not modify the voltage-dependence of steady-state inactivation (control $V_{1/2}$: -77.3 ± 1.2 mV vs GS967: -77.5 ± 1.3 mV; P = 0.45; n = 7 and 10 respectively; Supplemental Fig. S3).

The LQTS-associated $Na_V1.5$ mutation delKPQ exhibits enhanced I_{NaL} providing a more robust target for testing effects of GS967. Figure 1C illustrates that GS967 preferentially blocks delKPQ I_{NaL} significantly more than I_{NaP} (69.7% vs 34.8 inhibition, respectively, P

Molecular Pharmacology Fast Forward. Published on May 2, 2016 as DOI: 10.1124/mol.116.103358
This article has not been copyedited and formatted. The final version may differ from this version.

< 0.001; Fig. 1B and C), and the compound nearly eliminates aberrant inward current evoked by slow voltage ramps (Fig. 1D). Notably, GS967 suppresses delKPQ I_{NaP} to a greater extent than WT I_{NaP} (34.8% vs 18.6% inhibition; $P < 0.005$) illustrating a lower degree of selectivity for late over peak current for this LQTS mutation. This difference in I_{NaP} between WT and mutant $Na_V1.5$ was not due to differences in the rates of current 'rundown'. This observation suggested that peak current block by GS967 was context specific, and motivated us to examine other effects of GS967 on $Na_V1.5$ channels under different conditions, including a UDB paradigm.

Use-dependent block of $Na_V1.5$ by GS967

To test for UDB of $Na_V1.5$ by GS967, we applied a series of 50 short depolarizing pulses (20 ms) to -20 mV at different frequencies (0.5, 1, 2, 10 and 20 Hz). In the absence of GS967, there was no discernable loss of channel availability at stimulation frequencies of 0.5, 1 or 2 Hz, whereas at 10 and 20-Hz there was a ~20% reduction in channel availability (Fig. 2B). Following bath application of 1 μM GS967, repetitive pulsing was associated with a progressive reduction of $Na_V1.5$ I_{NaP} consistent with UDB of the channel (Fig. 2A and B). Use-dependent block of $Na_V1.5$ delKPQ I_{NaP} by 1 μM GS967 was not significantly different than that observed for WT channels at 2 and 10 Hz. However at 20 Hz, GS967 showed greater UDB of delKPQ I_{NaP} compared to WT channels (Supplemental Fig. S4). Use-dependent block of WT or mutant cardiac sodium channels by GS967 was not examined previously (Alves Bento et al., 2015; Belardinelli et al., 2013; Bonatti et al., 2014; Burashnikov et al., 2015; Carneiro et al., 2015).

Molecular Pharmacology Fast Forward. Published on May 2, 2016 as DOI: 10.1124/mol.116.103358
This article has not been copyedited and formatted. The final version may differ from this version.

We compared UDB of $Na_V1.5$ by GS967 against lidocaine, a known use-dependent sodium channel blocker (Huang et al., 2012) and another selective I_{NaL} blocker, ranolazine (Antzelevitch et al., 2014). Using automated patch clamp recording, we examined UDB of $Na_V1.5$ across a 1000-fold concentration range for GS967 and lidocaine but only a 100-fold concentration range for ranolazine due to poor solubility at high concentrations. All compounds exhibited UDB of I_{NaP} that was potentiated at higher pulsing frequencies (Fig. 3, Supplemental Fig. S5). At all frequencies, GS967 exhibited a similar block as lidocaine but with greater potency (140- to 320-fold lower IC_{50}).

GS967 impairs recovery from inactivation

To explore plausible mechanisms to explain the UDB of $Na_V1.5$ by GS967, we first examined recovery from fast and slow inactivation. This was done by utilizing a standard two-pulse protocol consisting of a depolarizing (-20 mV) 20 ms or 1000 ms pulse to engage fast or slow inactivation, respectively, followed by a variable duration recovery step to -120 mV and a final test pulse (-20 mV, 20 ms). Channel availability after the end of the recovery interval was normalized to initial values and plotted against the recovery time (Fig. 4A).

The time course of recovery from fast inactivation in the absence of GS967 exhibited a mono-exponential time course described by a single time constant (τ = 3.2 ± 0.3 ms), whereas in the presence of GS967, recovery exhibited a bi-exponential time course with a fast component, which was significantly larger than that observed in the absence of the compound (τ_{fast} = 5.2 ± 0.7 ms; $P < 0.001$), and a prominent slow component (τ_{slow} =

Molecular Pharmacology Fast Forward. Published on May 2, 2016 as DOI: 10.1124/mol.116.103358
This article has not been copyedited and formatted. The final version may differ from this version.

602.1 ± 77.5 ms) that represented 57.2 ± 2.8% of the recovering current (Fig. 4A, Table 1). The time course of recovery from slow inactivation was bi-exponential in both, the absence or presence of GS967. In the absence of GS967, recovery from slow inactivation was described by fast (τ_{fast} = 3.7 ± 0.3 ms) and slow time constants (τ_{slow} = 238.5 ± 26.8 ms) with relative weights of 68 ± 2.5% (fast) and 32 ± 2.5% (slow). GS967 significantly affected both fast and slow time constants and increased the relative weight of the slow component to 95 ± 1.0% (Fig. 4A, Table 1). A very similar effect of GS967 on recovery from inactivation of delKPQ channels was also observed (Supplemental Fig. S6; Table 1). These results suggest that GS967 can significantly impair recovery from both fast and slow inactivation.

GS967 enhances slow inactivation

Use-dependent block can also be due to accumulation of channels in a slow inactivated state evoked by prolonged membrane depolarization. We investigated whether kinetic differences in the rate of entry into slow inactivation could account for the UDB of $Na_V1.5$ by GS967. To assess the onset of slow inactivation, cells were held at -120 mV and then depolarized to -20 mV for a variable duration (2-1000 ms) followed by a brief recovery pulse (-120 mV for 20 ms) and a final 20 ms test pulse to -20 mV (voltage protocol illustrated in Fig. 4B). Mono-exponential fits were performed to determine the time constants for the onset of slow inactivation in the absence and presence of 1 µM GS967. In the absence of GS967, the time constant was 475.6 ± 29.7 ms, whereas in the presence of 1 µM GS967 the time constant for the onset of slow inactivation was significantly smaller (τ = 28.8 ± 2.6 ms; $P < 0.001$; Fig. 4B; Table 1) indicating that

Molecular Pharmacology Fast Forward. Published on May 2, 2016 as DOI: 10.1124/mol.116.103358
This article has not been copyedited and formatted. The final version may differ from this version.

$Na_V1.5$ channels entered the slow inactivated state more rapidly in the presence of GS967. These kinetic differences likely contribute to UDB by GS967 (Fig. 2). A very similar effect of GS967 on slow inactivation of delKPQ channels was also observed (Supplemental Fig. S6; Table 1).

Using the same protocol as in Fig. 4B, we observed that GS967 had a more potent effect than lidocaine and ranolazine to reduce I_{NaP} after long depolarizations (Supplemental Fig. S7). The calculated IC_{50} for GS967 was 30 nM, 200 and 1300 times lower than for lidocaine (IC_{50} = 6 µM) or ranolazine (IC_{50} = 41 µM), respectively (Fig. 5). These differences might be attributed to greater magnitude of effects on slow inactivation or due to differences in effects on recovery from inactivation (Lenkey et al., 2006).

GS967 effect requires a local anesthetic interaction site

Many features of $Na_V1.5$ block by GS967, including suppression of I_{NaL} and UDB of I_{NaP}, resemble effects of local anesthetic (LA) agents (Liu et al., 2003; Nagatomo et al., 2000). We examined whether the actions of GS967 depend upon a known LA interaction site in the D4/S6 segment (Catterall, 2014) by testing this compound on $Na_V1.5$ channels with a mutation (F1760A) at this site. Similar to WT channels, GS967 (1 µM) inhibited I_{NaL} to a significantly greater extent than I_{NaP} (10.9 ± 2 vs 73.2 ± 4%) at slow pulsing frequency (0.2 Hz. Fig. 6A and B). Moreover, the effect of GS967 on I_{NaL} was not statistically different between WT and F1760A channels (62.0 ± 7.0 vs 73.2 ± 4.0% inhibition respectively; P = 0.44). Further, GS967 significantly suppressed ramp-

Molecular Pharmacology Fast Forward. Published on May 2, 2016 as DOI: 10.1124/mol.116.103358
This article has not been copyedited and formatted. The final version may differ from this version.

currents evoked in F1760A expressing cells with a 5-fold suppression of net charge movement (Fig. 6C). Together, these results suggest that phenyalanine-1760 is not a critical determinant of I_{NaL} block by GS967.

We further assessed whether F1760A modifies UDB of I_{NaP} by GS967. First, we compared the intrinsic frequency-dependent loss of channel availability between F1760A and WT $Na_V1.5$ recorded in the absence of the compound. The F1760A mutation exhibits a lower level of intrinsic 'run down' at higher frequencies (10 and 20 Hz) than the WT channel (Supplemental Fig. S8). After bath application of 1 μM GS967, repetitive pulsing was associated with a progressive reduction of F1760A I_{NaP} consistent with UDB of the mutant channel at all frequencies (Fig. 7A). However, the degree of UDB of F1760A channels was significantly less than WT channels at 1 Hz or higher pulsing frequencies (Fig. 7B). Collectively, these data suggest that modification of the D4/S6 segment LA interaction site only partially attenuates UDB of I_{NaP} by GS967.

Finally, we examined the effect of the F1760A mutation on recovery from fast and slow inactivation. Figure 8 illustrates that F1760A has a slightly faster recovery from slow inactivation compared to the WT in the absence of the compound. GS967 significantly impairs F1760A recovery from slows inactivation but to a lesser extent than for WT $Na_V1.5$ (Fig. 8A and B; Table 1). This effect could be explained by a reduced slow time constant for recovery from inactivation and a smaller relative weight of this component. Similar to WT channels, GS967 also evoked an additional slow component for recovery from fast inactivation that was not observed in the absence of the compound, but this

Molecular Pharmacology Fast Forward. Published on May 2, 2016 as DOI: 10.1124/mol.116.103358
This article has not been copyedited and formatted. The final version may differ from this version.

slow component had a smaller amplitude and faster kinetics than WT channels (Table 1). GS967 dampened the extent of F1760A slow inactivation but the rate of onset of inactivation was not significantly different from WT $Na_V1.5$ (Fig. 8C; Table 1). These results suggest that mutation of the D4/S6 LA interaction site partially attenuates the effect of GS967 on onset and recovery from inactivation and this can explain less UDB. However, the effect of GS967 on F1760A was not complete and therefore there may be other channel regions important for the full actions of this compound.

Molecular Pharmacology Fast Forward. Published on May 2, 2016 as DOI: 10.1124/mol.116.103358
This article has not been copyedited and formatted. The final version may differ from this version.

DISCUSSION

In this study, we investigated the modulation of human $Na_V1.5$ by GS967, a recently described sodium channel blocker with potent antiarrhythmic effects in various *in vitro* and *in vivo* models. The antiarrhythmic effect of GS967 was previously attributed to preferential suppression of I_{NaL} (Belardinelli et al., 2013; Burashnikov et al., 2015; Pezhouman et al., 2014), but here we offer evidence for other potentially important biophysical effects on the human cardiac sodium channel. Specifically, we demonstrate that GS967 exerts a previously unreported strong effect on slow inactivation and recovery from inactivation resulting in substantial UDB. These revelations may help explain the pharmacological effects of GS967 in arrhythmia models and other settings.

Initially, we confirmed that GS967 applied to heterologously expressed human $Na_V1.5$ does indeed exhibit significantly greater tonic block of I_{NaL} than I_{NaP} without modifying inactivation kinetics. This effect was more evident in cells expressing the LQTS mutation delKPQ, which has a greater amplitude of I_{NaL} than observed for WT-$Na_V1.5$ channels. Importantly, we also demonstrated that GS967 exerts a strong UDB with IC_{50} values ranging from 70 to 100 nM depending on stimulation frequency. GS967 exerts a qualitatively similar UDB of $Na_V1.5$ to that of lidocaine, a prototypic use-dependent blocker of sodium channels, but with significantly greater potency. The basis for UDB by GS967 is most likely a previously unreported strong effect on slow inactivation and recovery from inactivation. The strong UDB exerted by GS967 may contribute to its observed antiarrhythmic efficacy.

Molecular Pharmacology Fast Forward. Published on May 2, 2016 as DOI: 10.1124/mol.116.103358
This article has not been copyedited and formatted. The final version may differ from this version.

It was initially reported that GS967 reduces the pro-arrhythmic consequences of enhanced I_{NaL} in rabbit models of reduced repolarization reserve and ischemia involving ventricular myocardium (Belardinelli et al., 2013). GS967 was also shown to suppress atrial arrhythmogenicity evoked by ATX-II, E-4031 or catecholamines (Sicouri et al., 2013). More recent reports highlight the antiarrhythmic effects of GS967 in other models of either ventricular or atrial arrhythmia. GS967 was demonstrated to suppress EADs and DADs as well as to prevent ventricular tachyarrhythmia in rat hearts exposed to aconitine or hydrogen peroxide (Pezhouman et al., 2014). Bonatti and colleagues observed prevention of ischemia-induced depolarization and repolarization abnormalities in both atria and ventricles of pigs with acute coronary artery stenosis by GS967 whereas flecainide potentiated the proarrhythmic effects of acute ischemia (Bonatti et al., 2014). GS967 also prevented hypokalemia-induced ventricular fibrillation in rats and rabbits (Pezhouman et al., 2014), catecholamine-induced ventricular tachycardia in pigs (Alves Bento et al., 2015) and prevents chemically-induced spontaneous atrial fibrillation in a porcine model (Carneiro et al., 2015). All of these effects were observed with GS967 levels in the range of 0.3-1 μM, which is sufficient to suppress I_{NaL} but also to evoke UDB, allowing us to speculate that antiarrhythmic effects of this compound may be due to the combination of I_{NaL} suppression and UDB.

In this study we also demonstrated that GS967 also suppresses I_{NaL} conducted by the LQTS mutation delKPQ. As a result, GS967 nearly eliminates the aberrant inward current evoked by slow voltage ramps. Use-dependent block of $Na_V1.5$ delKPQ I_{NaP} by GS967 at low frequencies was not significantly different than that observed for WT

Molecular Pharmacology Fast Forward. Published on May 2, 2016 as DOI: 10.1124/mol.116.103358
This article has not been copyedited and formatted. The final version may differ from this version.

channels. The ability for GS967 to target I_{NaL} and to produce a significant UDB in the context of LQT3 mutations suggest that compounds sharing these functional properties of GS967 may be useful in the treatment of arrhythmias for LQTS-associated $Na_V1.5$ mutations. Indeed, another selective I_{NaL} (GS6615, eleclazine) is undergoing clinical trials for type 3 LQTS (Gilead, 2000-2015). Whether GS6615 also exerts effects on slow inactivation and evokes UDB awaits further study.

Slow inactivation influences cellular excitability, particularly in pathophysiological conditions associated with prolonged membrane repolarization such as epilepsy (Fleidervish et al., 1996), neuronal or cardiac ischemia (Shander et al., 1995), arrhythmias (Veldkamp et al., 2000) and neuromuscular channelopathies (Cannon, 1996). By accelerating the onset of slow inactivation and impairing recovery from inactivation of cardiac sodium channels, GS967 might increase the post-repolarization refractoriness (PRR), prevent premature membrane excitation and enable antiarrhythmic as well as anticonvulsant efficacy. In separate work, we recently demonstrated antiepileptic effects of GS967 in two mouse models (Anderson et al., 2014) and further work is needed to determine if UDB of neuronal sodium channels contributes to this effect.

Antiarrhythmic drugs with local anesthetic-like properties preferentially target the inactivated state of sodium channels and likely interact with a highly conserved local anesthetic (LA) drug receptor formed by residues from multiple S6 segments (Catterall, 2014). While many features of $Na_V1.5$ inhibition by GS967, including suppression of I_{NaL}

Molecular Pharmacology Fast Forward. Published on May 2, 2016 as DOI: 10.1124/mol.116.103358
This article has not been copyedited and formatted. The final version may differ from this version.

and UDB of I_{NaP}, resemble effects of LA agents (Belardinelli et al., 2013; Liu et al., 2003), we found that phenyalanine-1760 was not a critical determinant of tonic I_{NaL} block by GS967. By contrast, mutation of the D4/S6 LA interaction site attenuates the effect of GS967 on onset and recovery from inactivation and reduces UDB. It has been suggested that phenyalanine-1760 contributes to slow inactivation and links drug action to slow inactivation (Carboni et al., 2005). However, the effect of F1760A on UDB was not complete and therefore there may be other channel regions important for the full actions of GS967. We can conclude that the mode of action of GS967 is somewhat distinct from LA and that the block of I_{NaL} and I_{NaP} by GS967 does not entirely depend on the known LA drug receptor.

In conclusion, our study demonstrated that GS967 affects multiple biophysical properties of human $Na_V1.5$. Specifically, GS967 exerts strong UDB most likely because of high affinity binding of GS967 to $Na_V1.5$ inactivated states, by accelerating entry into slow inactivation and impairing recovery from inactivation. GS967 is a more potent use-dependent blocker than the antiarrhythmic drugs lidocaine and ranolazine. GS967 ability to inhibit specifically I_{NaL} over I_{NaP} and its newly described ability to evoke UDB may contribute to its antiarrhythmic effects.

Molecular Pharmacology Fast Forward. Published on May 2, 2016 as DOI: 10.1124/mol.116.103358
This article has not been copyedited and formatted. The final version may differ from this version.

ACKNOWLEDGMENTS

The authors thank Reshma Desai for her technical assistance.

AUTHORSHIP CONTRIBUTIONS

Participated in research design: Potet and George.

Conducted experiments: Potet and Vanoye.

Performed data analysis: Potet.

Wrote or contributed to the writing of the manuscript: Potet, Vanoye and George.

REFERENCES

Alves Bento AS, Bacic D, Saran Carneiro J, Nearing BD, Fuller H, Justo FA, Rajamani S, Belardinelli L and Verrier RL (2015) Selective late INa inhibition by GS-458967 exerts parallel suppression of catecholamine-induced hemodynamically significant ventricular tachycardia and T-wave alternans in an intact porcine model. *Heart Rhythm* **12**(12): 2508-2514.

Anderson LL, Thompson CH, Hawkins NA, Nath RD, Petersohn AA, Rajamani S, Bush WS, Frankel WN, Vanoye CG, Kearney JA and George AL, Jr. (2014) Antiepileptic activity of preferential inhibitors of persistent sodium current. *Epilepsia* **55**(8): 1274-1283.

Antzelevitch C, Nesterenko V, Shryock JC, Rajamani S, Song Y and Belardinelli L (2014) The role of late I Na in development of cardiac arrhythmias. *Handb Exp Pharmacol* **221**: 137-168.

Belardinelli L, Liu G, Smith-Maxwell C, Wang WQ, El-Bizri N, Hirakawa R, Karpinski S, Li CH, Hu L, Li XJ, Crumb W, Wu L, Koltun D, Zablocki J, Yao L, Dhalla AK, Rajamani S and Shryock JC (2013) A novel, potent, and selective inhibitor of cardiac late sodium current suppresses experimental arrhythmias. *J Pharmacol Exp Ther* **344**(1): 23-32.

Bennett PB, Yazawa K, Makita N and George AL, Jr. (1995) Molecular mechanism for an inherited cardiac arrhythmia. *Nature* **376**(6542): 683-685.

Bonatti R, Silva AF, Batatinha JA, Sobrado LF, Machado AD, Varone BB, Nearing BD, Belardinelli L and Verrier RL (2014) Selective late sodium current blockade with GS-458967 markedly reduces ischemia-induced atrial and ventricular repolarization alternans and ECG heterogeneity. *Heart Rhythm* **11**(10): 1827-1835.

Burashnikov A, Di Diego JM, Goodrow RJ, Jr., Belardinelli L and Antzelevitch C (2015) Atria are More Sensitive Than Ventricles to GS-458967-Induced Inhibition of Late Sodium Current. *J Cardiovasc Pharmacol Ther* **20**(5): 501-508.

Cannon SC (1996) Slow inactivation of sodium channels: more than just a laboratory curiosity. *Biophys J* **71**(1): 5-7.

Carboni M, Zhang ZS, Neplioueva V, Starmer CF and Grant AO (2005) Slow sodium channel inactivation and use-dependent block modulated by the same domain IV S6 residue. *J Membr Biol* **207**(2): 107-117.

Carneiro JS, Bento AS, Bacic D, Nearing BD, Rajamani S, Belardinelli L and Verrier RL (2015) The Selective Cardiac Late Sodium Current Inhibitor GS-458967 Suppresses Autonomically Triggered Atrial Fibrillation in an Intact Porcine Model. *J Cardiovasc Electrophysiol* **26**(12): 1364-1369.

Catterall WA (2014) Structure and function of voltage-gated sodium channels at atomic resolution. *Exp Physiol* **99**(1): 35-51.

Fleidervish IA, Friedman A and Gutnick MJ (1996) Slow inactivation of Na+ current and slow cumulative spike adaptation in mouse and guinea-pig neocortical neurones in slices. *J Physiol* **493 (Pt 1)**: 83-97.

Gilead (2000-2015) Gilead Sciences: Effect of Eleclazine on Shortening of the QT Interval, Safety, and Tolerability in Adults With Long QT Syndrome Type 3. *In: ClinicalTrialsgov [Internet] Bethesda (MD): National Library of Medicine (US)*:

Available from https://clinicaltrials.gov/show/NCT02300558 NLM identifier: NCT02300558.

Gupta T, Khera S, Kolte D, Aronow WS and Iwai S (2015) Antiarrhythmic properties of ranolazine: A review of the current evidence. *Int J Cardiol* **187**: 66-74.

Huang CJ, Schild L and Moczydlowski EG (2012) Use-dependent block of the voltage-gated Na(+) channel by tetrodotoxin and saxitoxin: effect of pore mutations that change ionic selectivity. *J Gen Physiol* **140**(4): 435-454.

Koltun DO, Parkhill EQ, Elzein E, Kobayashi T, Notte GT, Kalla R, Jiang RH, Li X, Perry TD, Avila B, Wang WQ, Smith-Maxwell C, Dhalla AK, Rajamani S, Stafford B, Tang J, Mollova N, Belardinelli L and Zablocki JA (2016) Discovery of triazolopyridine GS-458967, a late sodium current inhibitor (Late Ii) of the cardiac Na 1.5 channel with improved efficacy and potency relative to ranolazine. *Bioorg Med Chem Lett*.

Le Grand B, Vie B, Talmant JM, Coraboeuf E and John GW (1995) Alleviation of contractile dysfunction in ischemic hearts by slowly inactivating Na+ current blockers. *Am J Physiol* **269**(2 Pt 2): H533-540.

Lenkey N, Karoly R, Kiss JP, Szasz BK, Vizi ES and Mike A (2006) The mechanism of activity-dependent sodium channel inhibition by the antidepressants fluoxetine and desipramine. *Mol Pharmacol* **70**(6): 2052-2063.

Liu H, Atkins J and Kass RS (2003) Common molecular determinants of flecainide and lidocaine block of heart Na+ channels: evidence from experiments with neutral and quaternary flecainide analogues. *J Gen Physiol* **121**(3): 199-214.

Maltsev VA and Undrovinas A (2008) Late sodium current in failing heart: friend or foe? *Prog Biophys Mol Biol* **96**(1-3): 421-451.

Nagatomo T, January CT and Makielski JC (2000) Preferential block of late sodium current in the LQT3 DeltaKPQ mutant by the class I(C) antiarrhythmic flecainide. *Mol Pharmacol* **57**(1): 101-107.

Pezhouman A, Madahian S, Stepanyan H, Ghukasyan H, Qu Z, Belardinelli L and Karagueuzian HS (2014) Selective inhibition of late sodium current suppresses ventricular tachycardia and fibrillation in intact rat hearts. *Heart Rhythm* **11**(3): 492-501.

Pignier C, Rougier JS, Vie B, Culie C, Verscheure Y, Vacher B, Abriel H and Le Grand B (2010) Selective inhibition of persistent sodium current by F 15845 prevents ischaemia-induced arrhythmias. *Br J Pharmacol* **161**(1): 79-91.

Ruan Y, Liu N and Priori SG (2009) Sodium channel mutations and arrhythmias. *Nat Rev Cardiol* **6**(5): 337-348.

Shander GS, Fan Z and Makielski JC (1995) Slowly recovering cardiac sodium current in rat ventricular myocytes: effects of conditioning duration and recovery potential. *J Cardiovasc Electrophysiol* **6**(10 Pt 1): 786-795.

Sicouri S, Antzelevitch D, Heilmann C and Antzelevitch C (1997) Effects of sodium channel block with mexiletine to reverse action potential prolongation in in vitro models of the long term QT syndrome. *J Cardiovasc Electrophysiol* **8**(11): 1280-1290.

Sicouri S, Belardinelli L and Antzelevitch C (2013) Antiarrhythmic effects of the highly selective late sodium channel current blocker GS-458967. *Heart Rhythm* **10**(7): 1036-1043.

Song Y, Shryock JC and Belardinelli L (2008) An increase of late sodium current induces delayed afterdepolarizations and sustained triggered activity in atrial myocytes. *Am J Physiol Heart Circ Physiol* **294**(5): H2031-2039.

Song Y, Shryock JC, Wagner S, Maier LS and Belardinelli L (2006) Blocking late sodium current reduces hydrogen peroxide-induced arrhythmogenic activity and contractile dysfunction. *J Pharmacol Exp Ther* **318**(1): 214-222.

Song Y, Shryock JC, Wu L and Belardinelli L (2004) Antagonism by ranolazine of the pro-arrhythmic effects of increasing late INa in guinea pig ventricular myocytes. *J Cardiovasc Pharmacol* **44**(2): 192-199.

Sossalla S, Kallmeyer B, Wagner S, Mazur M, Maurer U, Toischer K, Schmitto JD, Seipelt R, Schondube FA, Hasenfuss G, Belardinelli L and Maier LS (2010) Altered Na(+) currents in atrial fibrillation effects of ranolazine on arrhythmias and contractility in human atrial myocardium. *J Am Coll Cardiol* **55**(21): 2330-2342.

Veldkamp MW, Viswanathan PC, Bezzina C, Baartscheer A, Wilde AA and Balser JR (2000) Two distinct congenital arrhythmias evoked by a multidysfunctional Na(+) channel. *Circ Res* **86**(9): E91-97.

Wu L, Ma J, Li H, Wang C, Grandi E, Zhang P, Luo A, Bers DM, Shryock JC and Belardinelli L (2011) Late sodium current contributes to the reverse rate-dependent effect of IKr inhibition on ventricular repolarization. *Circulation* **123**(16): 1713-1720.

FOOTNOTES

This work was supported by a Scientist Development Grant [11SDG5330006] from the American Heart Association (F.P.) and a research grant from Gilead Sciences, Inc.

DISCLOSURES

The work was partially supported by a research grant from Gilead Sciences, Inc.

Molecular Pharmacology Fast Forward. Published on May 2, 2016 as DOI: 10.1124/mol.116.103358
This article has not been copyedited and formatted. The final version may differ from this version.

LEGENDS FOR FIGURES

Figure 1. GS967 selectively inhibits $Na_V1.5$ I_{NaL}.

A, Representative TTX-subtracted I_{Na} from $Na_V1.5$-expressing cells in the absence (black) and presence (red) of 1 µM GS967. Cells were held at a membrane potential of -120 mV and depolarized every 4 seconds to -20 mV for 200 ms. **B,** Representative TTX-subtracted I_{Na} from cells expressing $Na_V1.5$-delKPQ in the absence (black) and presence (red) of 1 µM GS967. Cells were held at -120 mV and depolarized every 4 seconds to -20 mV for 200 ms. **C,** Summary of effects of 1 µM GS967 on WT and delKPQ I_{NaP} and I_{NaL}. GS967 caused a decrease of I_{NaP} and I_{NaL} by 18.6 ± 1.8% and 62 ± 6.9%, respectively (n = 16; $P < 0.001$) for WT, and 34.8 ± 4.0% and 69.7 ± 6.8%, respectively (n = 13; $P < 0.001$) for delKPQ. I_{NaL} was determined from TTX subtracted current over the final 10 ms of a 200 ms pulse to -20 mV and normalized to peak current. **D,** Normalized and averaged TTX-subtracted ramp-currents (0.09 mV/ms) recorded from cells expressing $Na_V1.5$-delKPQ in the absence (black) and presence (red) of 1 µM GS967 and expressed as a percentage of I_{NaP}. The net charge movement during voltage ramps was 9.2 ± 1.3 pC/nA in the absence and 2.1 ± 0.4 pC/nA in the presence of 1 µM GS967 (n = 12; $P < 0.001$). All data are presented as mean ± SEM.

Figure 2. Use-dependent block of human $Na_V1.5$ by GS967.

To examine use-dependent block, cells were held at -120 mV and pulsed to -20 mV for 20 ms at five different frequencies (0.5, 1, 2, 10 and 20 Hz), with an inter-pulse potential of -120 mV (see inset). The peak currents elicited by each pulse were normalized to the peak current of first pulse and plotted against the pulse number. Black symbols

represent absence of drug, while gray symbols represent experiments in the presence of 1 µM GS967. **A,** Response of cells expressing the WT channels to 1 µM GS967 at 0.5, 1, 2, 10 and 20 Hz. **B,** Relative amplitudes at the last sweep (50^{th}) at 0.5, 1, 2, 10 and 20 Hz were 1.03 ± 0.01, 0.99 ± 0.01, 0.98 ± 0.01, 0.89 ± 0.01 and 0.77 ± 0.02 respectively, in the absence (black) of 1 µM GS967, and 0.92 ± 0.02 (n = 5; $P < 0.05$), 0.85 ± 0.02 (n = 5; $P < 0.05$), 0.68 ± 0.02 (n = 11; $P < 0.001$), 0.25 ± 0.01 (n = 18; $P < 0.001$) and 0.12 ± 0.01 (n = 18; $P < 0.001$) respectively, in the presence (gray) of 1 µM GS967. All data are presented as mean ± SEM.

Figure 3. Concentration-dependence of $Na_V1.5$ use-dependent block by GS967, ranolazine and lidocaine.

Concentration-response relationships for use-dependent block at 3 different pulsing frequencies (2, 10 and 20 Hz) were determined as the amplitude of current evoked by the 50th pulse normalized to that of the current evoked by the first pulse plotted as a function of drug concentration. Recordings were performed using automated planar patch-clamp and HEK-293 cells stably expressing human $Na_V1.5$. **A,** Concentration-response relationships for the use-dependent block at 2 Hz. IC_{50} = 0.1, 34 and 14 µM for GS967, ranolazine and lidocaine respectively. **B,** Concentration-response for use-dependent block at 10 Hz. IC_{50} = 0.1, 22 and 32 µM for GS967, ranolazine and lidocaine respectively. **C,** Concentration-response for use-dependent block at 20 Hz. IC_{50} = 0.07, 17 and 16 µM for GS967, ranolazine and lidocaine respectively. Data represent mean ± SEM; the number of experiments for each concentration is indicated next to the corresponding data points. Values of IC_{50} are also indicated on each plot.

Molecular Pharmacology Fast Forward. Published on May 2, 2016 as DOI: 10.1124/mol.116.103358
This article has not been copyedited and formatted. The final version may differ from this version.

Figure 4. GS967 modifies $Na_V1.5$ onset of and recovery from inactivation.

A, Recovery from slow (1000 ms step, circles) and fast (20 ms step, triangles) inactivation determined in the absence (black) or presence (gray) of 1 μM GS967. Recovery from slow inactivation exhibited a bi-exponential time course with fast and slow time constants (time constant values and relative weights are provided in Table 1). The recovery from fast inactivation was mono-exponential in the absence and bi-exponential in presence of 1 μM GS967 (time constant values and relative weights are provided in Table 1). **B,** Onset of slow inactivation was determined in the absence (black) and presence of 1 μM GS967 (gray) using a two-pulse protocol (inset). The time constants for onset of slow inactivation are provided in Table 1. All data are presented as mean ± SEM.

Figure 5. Concentration-dependence of $Na_V1.5$ onset of slow inactivation by GS967, ranolazine and lidocaine.

Concentration-response relationships for the onset of slow inactivation induced by GS967, ranolazine and lidocaine were determined by automated patch clamp recording from cells stably expressing human $Na_V1.5$ using the two-pulse protocol illustrated in Fig. 4B. Concentration-response curves for the onset of slow inactivation induced by GS967 (black) ranolazine (blue) and lidocaine (red) were fitted to a four parameter sigmoidal equation and the IC_{50} for each drug or compound was determined. GS967, ranolazine and lidocaine IC_{50} values were 0.03, 41 and 6 μM respectively. Data represent mean ± SEM; the number of experiments for each concentration is indicated next to the corresponding data point.

Molecular Pharmacology Fast Forward. Published on May 2, 2016 as DOI: 10.1124/mol.116.103358
This article has not been copyedited and formatted. The final version may differ from this version.

Figure 6. GS967 selectively inhibits $Na_V1.5$-F1760A I_{NaL}.

A, Representative TTX-subtracted I_{Na} from cells expressing $Na_V1.5$-F1760A in the absence (black) or presence (red) of 1 μM GS967. Cells were held at -120 mV and depolarized every 4 seconds to -20 mV for 200 ms. **B,** Summary of effects of 1 μM GS967 on WT and F1760A I_{NaP} and I_{NaL}. $Na_V1.5$-F1760A I_{NaP} and I_{NaL} were decreased by 10.9 ± 2.0% and 73.2 ± 4.0%, respectively (n = 14; $P < 0.001$). **C,** Normalized and averaged TTX-subtracted ramp-currents (0.09 mV/ms) recorded from cells expressing $Na_V1.5$-F1760A expressed as a percentage of peak I_{Na} in the absence (black) or presence of (red) 1 μM GS967. The net charge movement during voltage ramps was 9.4 ± 1.0 pC/nA in the absence and 1.8 ± 0.2 pC/nA in the presence of 1 μM GS967 (n = 14; $P < 0.001$). All data are presented as mean ± S.E.M.

Figure 7. Use-dependent block of $Na_V1.5$-F1760A by GS967.

Cells were held at –120 mV and pulsed to -20 mV (20 ms) at 5 different frequencies (0.5, 1, 2, 10 and 20 Hz), with inter-pulse potential set at -120 mV (see inset). The peak currents elicited by each pulse were normalized to the first pulse peak current then plotted against the pulse number. **A,** Response of cells expressing $Na_V1.5$-F1760A to 1 μM GS967 at 0.5, 1, 2, 10 and 20 Hz. **B,** Comparison of the relative amplitudes at the last sweep (50^{th}) of the use-dependent protocol for the WT (black) and F1760A mutant (gray) at 0.5, 1, 2, 10 and 20 Hz in presence of 1 μM GS967. Relative amplitudes at the last sweep (50^{th}) at 0.5, 1, 2, 10 and 20 Hz were 0.93 ± 0.02 (n = 5), 0.85 ± 0.02 (n = 5), 0.68 ± 0.02 (n = 11), 0.25 ± 0.01 (n = 18) and 0.12 ± 0.01 (n = 18) respectively, for the WT, and 0.98 ± 0.02 (n = 6; $P = 0.068$), 0.92 ± 0.01 (n = 6; $P < 0.05$), 0.84 ± 0.01 (n =

Molecular Pharmacology Fast Forward. Published on May 2, 2016 as DOI: 10.1124/mol.116.103358
This article has not been copyedited and formatted. The final version may differ from this version.

11; $P < 0.001$), 0.56 ± 0.01 (n = 15; $P < 0.001$) and 0.42 ± 0.01 (n = 15; $P < 0.001$) respectively, for F1760A. Data represent mean ± SEM.

Figure 8. GS967 affects $Na_V1.5$-F1760A onset of slow inactivation and recovery from inactivation.

Recovery from slow (1000 ms step; **A**) and fast (20 ms step, **B**) inactivation from cells expressing F1760A or WT $Na_V1.5$ determined in the absence (black) or presence (gray) of 1 µM GS967. The recovery from slow inactivation was bi-exponential in both the absence and presence of GS967 (see Table 1). F1760A recovery from fast inactivation was mono-exponential in absence and bi-exponential in presence of 1 µM GS967 (see Table 1). **C,** The onset of slow inactivation from cells expressing WT or F1760A $Na_V1.5$ in the absence (black) and presence of 1 µM GS967 (gray) was assessed using a two-pulse protocol (inset). F1760A onset of slow inactivation time constant was mono-exponential (see Table 1). Data represent mean ± SEM.

Molecular Pharmacology Fast Forward. Published on May 2, 2016 as DOI: 10.1124/mol.116.103358
This article has not been copyedited and formatted. The final version may differ from this version.

TABLES

Table 1. Effects of GS967 on WT $Na_V1.5$, delKPQ and F1760A onset and recovery from inactivation

	WT $Na_V1.5$		delKPQ		F1760A	
	Control	**1 μM GS967**	**Control**	**1 μM GS967**	**Control**	**1 μM GS967**
Recovery from slow Inactivation						
Relative weight (%)	68.6 ± 2.5	5.5 ± 1.0*	63.9 ± 2.9	13.6 ± 2.1*†	68.7 ± 1.4	28.8 ± 1.7*†
τ_{fast} (ms)	3.7 ± 0.3	9.2 ± 0.9*	3.4 ± 0.2	39.0 ± 11.1*†	3.6 ± 0.3	9.3 ± 0.7*
Relative weight (%)	31.4 ± 2.5	94.5 ± 1.0*	36.1 ± 2.9	86.4 ± 2.1*†	31.3 ± 1.4	71.2 ± 1.7*†
τ_{slow} (ms)	238.5 ± 26.8	600.8 ± 24.3*	224.0 ± 30.6	730.9 ± 62.2*†	107.1 ± 17.4†	373.3 ± 23.9*†
n	18	18	11	11	14	14
Recovery from fast Inactivation						
Relative weight (%)		42.8 ± 2.8		57.0 ± 4.8		62.5 ± 2.3†
τ_{fast} (ms)	3.2 ± 0.3	5.2 ± 0.7*	3.5 ± 0.2	4.9 ± 1.1	3.4 ± 0.2	4.9 ± 0.4*
Relative weight (%)		57.2 ± 2.8		43.0 ± 4.8†		37.5 ± 2.3†
τ_{slow} (ms)		602.1 ± 77.5		383.6 ± 86.0†		338.7 ± 40.2†
n	11	11	6	6	11	11
Onset of slow Inactivation						
τ(ms)	475.6 ± 29.7	28.8 ± 2.6*	549.0± 49.5	30.1 ± 2.8*	537.9 ± 70.4	31.1 ± 2.4*
n	16	16	12	12	14	14

*, $P < 0.05$ (compared to control condition).
†, $P < 0.05$ (compared to WT)

FIGURES

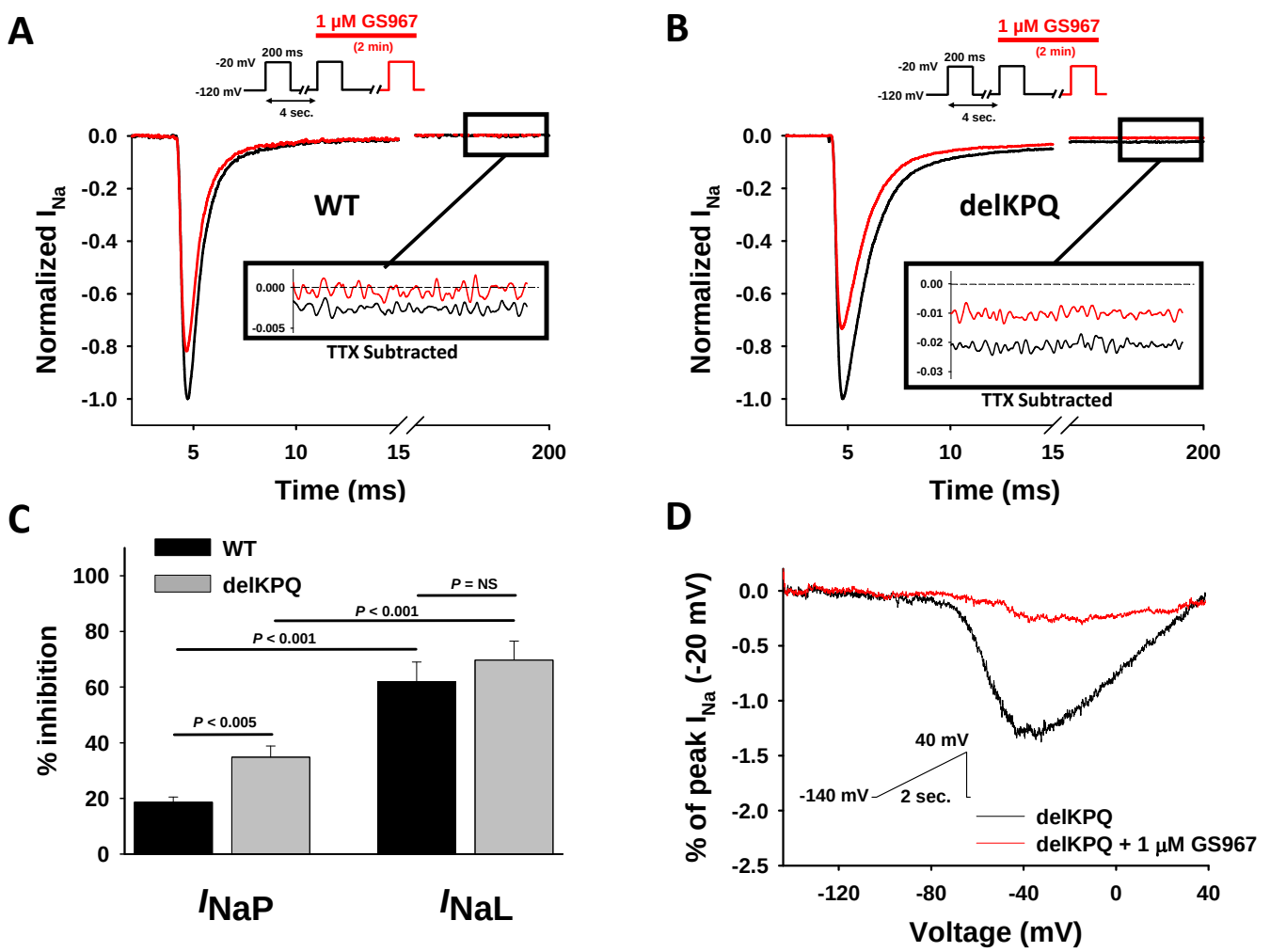

Figure 1

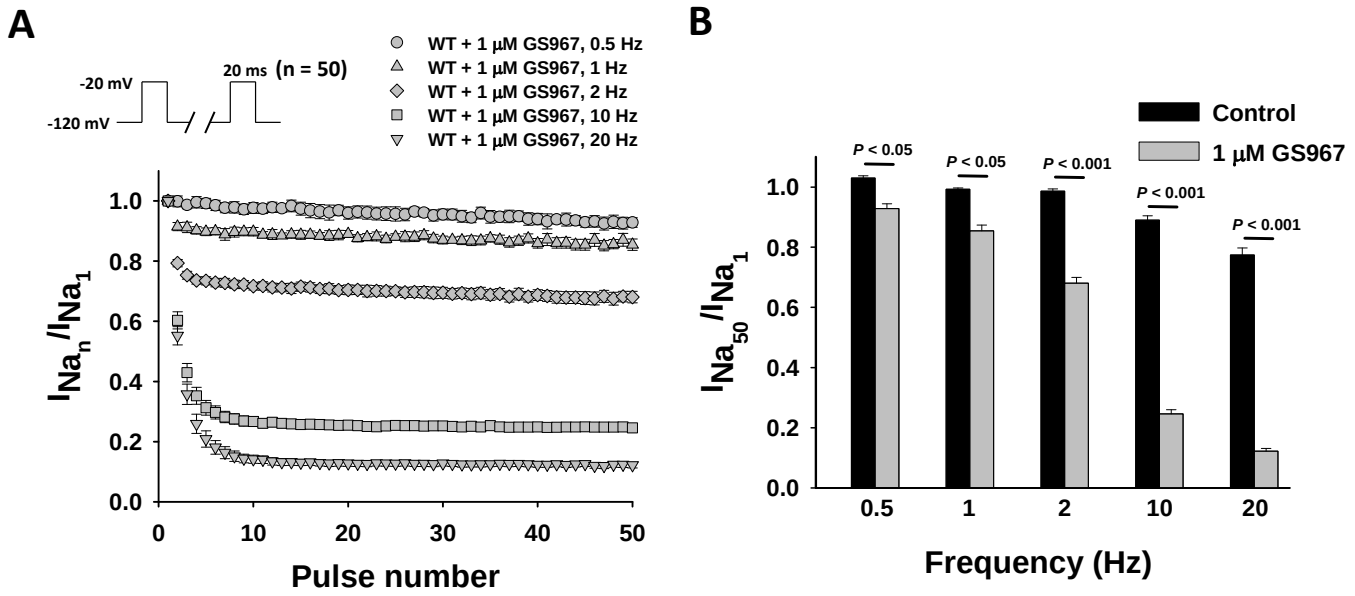

Figure 2

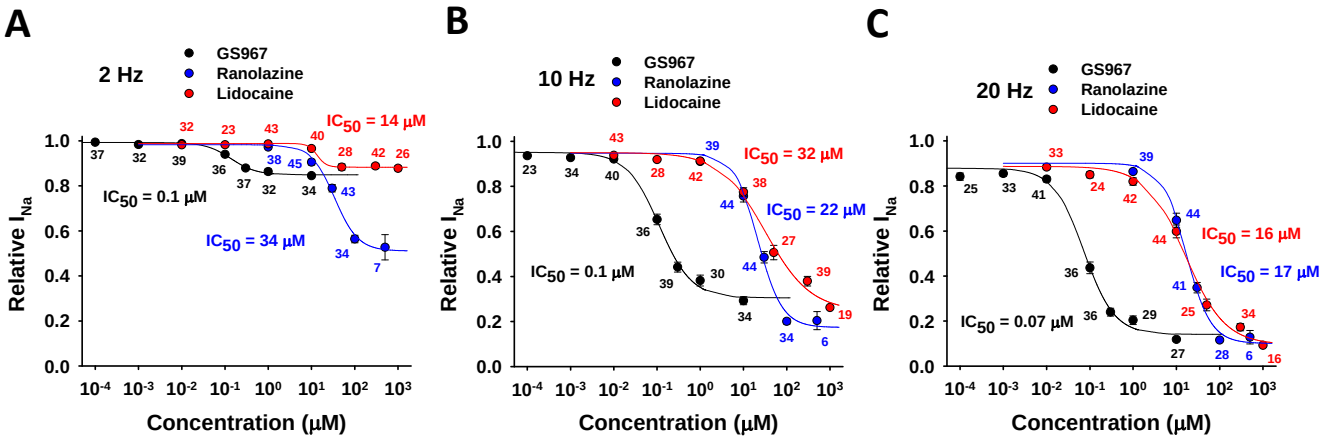

Figure 3

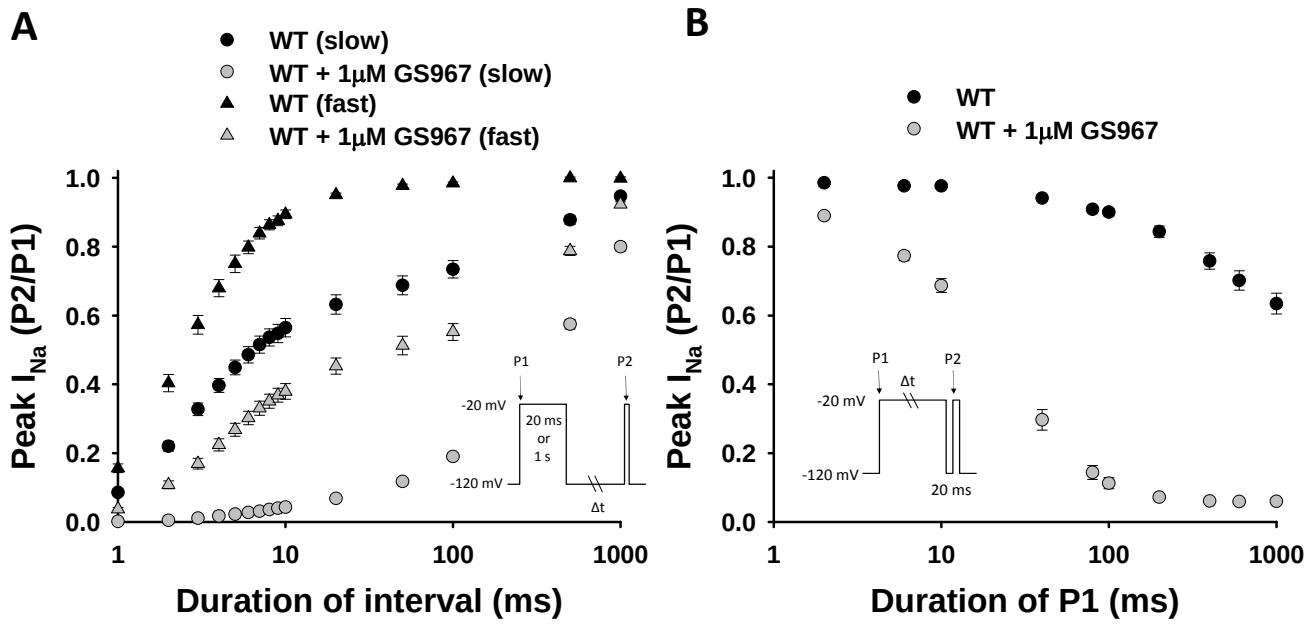

Figure 4

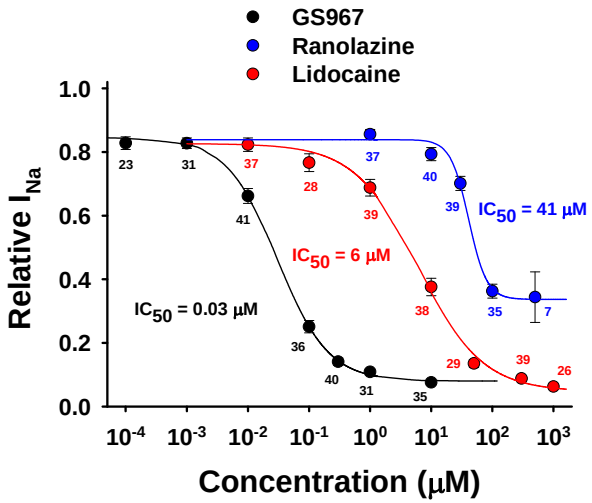

Figure 5

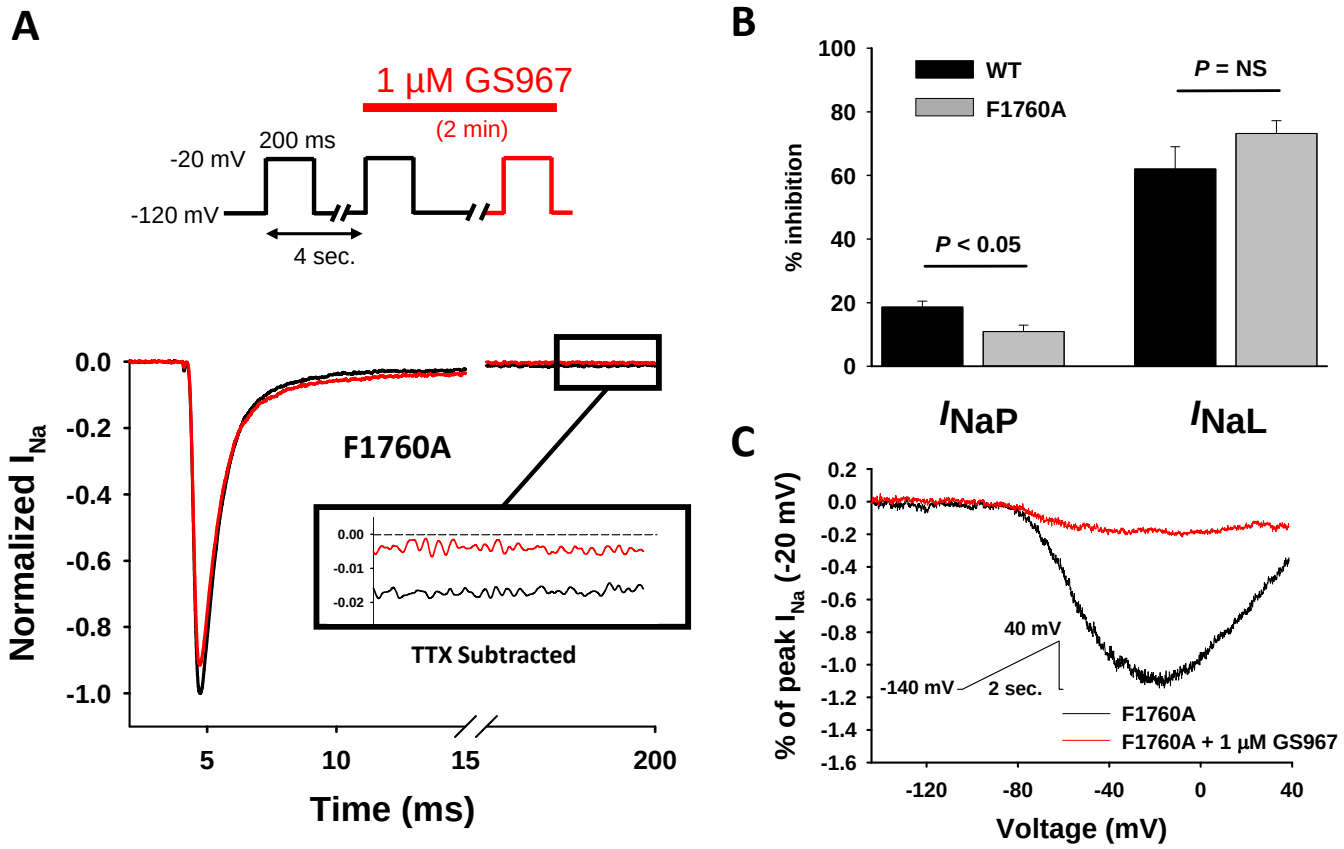

Figure 6

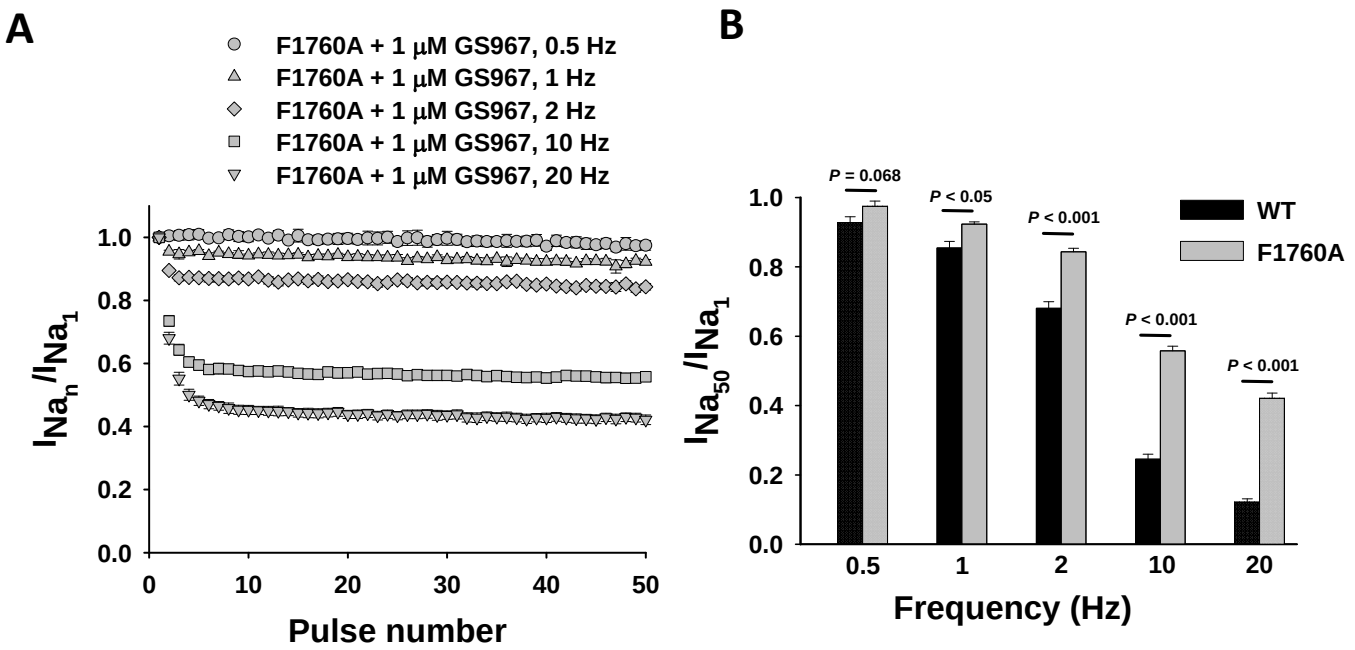

Figure 7

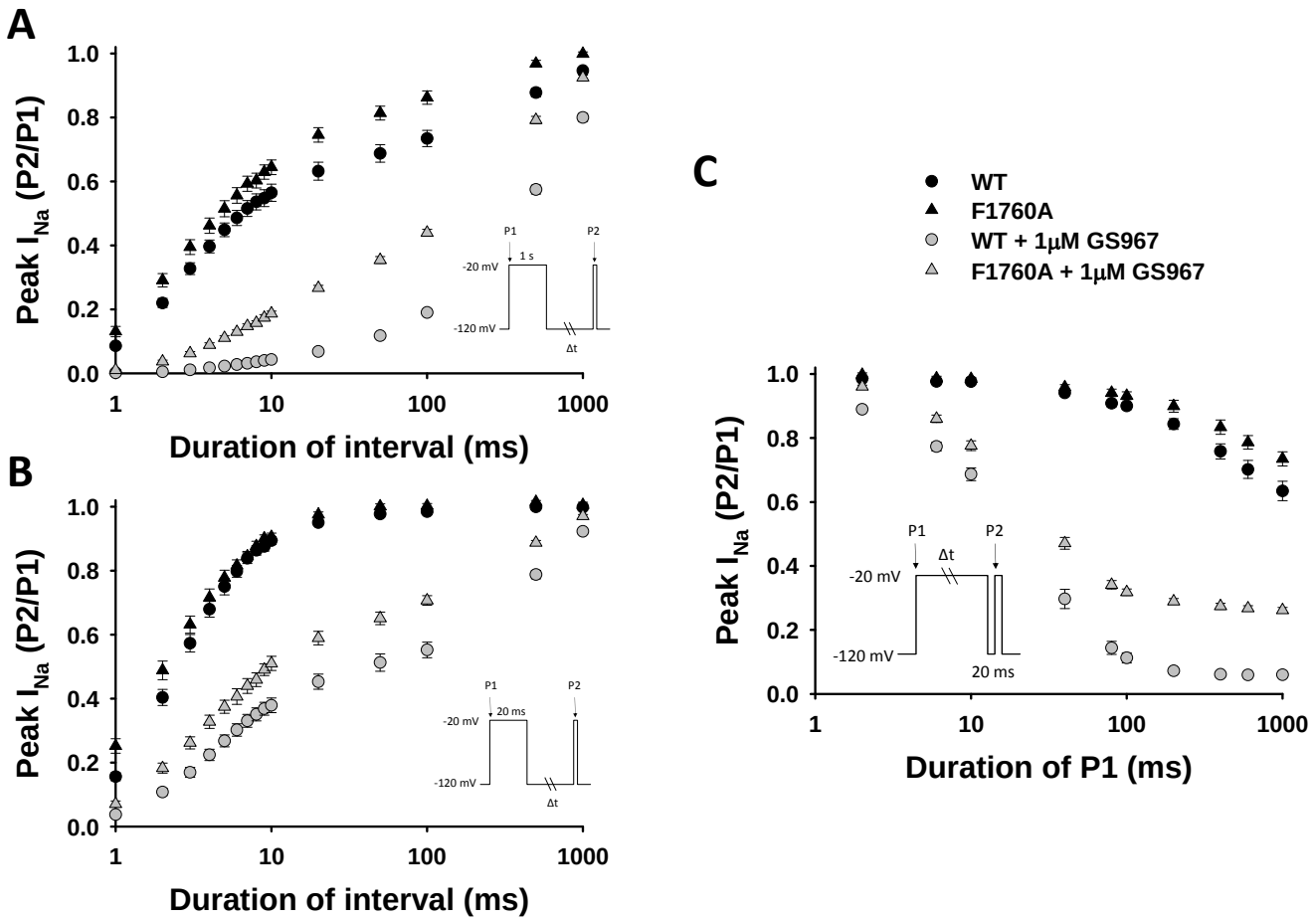

Figure 8